

IMPROVING PREDICTIONS FOR CAMBER IN PRECAST, PRESTRESSED CONCRETE BRIDGE GIRDERS

Michael A. Rosa, PE, Washington State Department of Transportation, Tumwater, WA
John F. Stanton, PhD, PE, Dept. of Civil and Environmental Engineering, University of
Washington, Seattle

Marc O. Eberhard, PhD, Dept. of Civil and Environmental Engineering, University of
Washington, Seattle

ABSTRACT

This paper provides recommendations for improving methods of predicting camber in prestressed concrete girders. A computer program was written to calculate camber as a function of time. It takes into account instantaneous and time-dependent behavior of the concrete and steel and performs the calculations in a series of time steps. The program was calibrated by comparing its predictions with the camber from 146 girders, measured in the fabricator's yard both after release and at a later time. Its long-term predictions were then compared with the responses of 91 girders that were monitored during construction at the Keys Road Bridge site in Yakima, Washington.

The calculated cambers were sensitive to the assumed prestress losses; for example, the 2007 AASHTO values for prestress loss provided much better camber estimates than did the 2004 provisions. In addition, the camber was found to depend most on the elastic modulus of the concrete, its creep coefficient, and the way that the prestress losses are incorporated into the calculation of the creep camber. To achieve the best match with the measured cambers, the AASHTO-recommended values for the elastic modulus and the creep coefficient had to be modified, and the prestress losses had to be taken into account when computing the time-dependant component of camber.

KEYWORDS: Camber, Deflection, Girder, Prestressed Concrete, Precast Concrete, Creep, Shrinkage, Elastic Modulus

INTRODUCTION

The Washington State Department of Transportation (WSDOT) has been using precast prestressed concrete girders in bridge applications for many years. These girders have allowed for longer spans, provided economical design, and accelerated construction schedules by allowing precast fabricators to deliver ready-made products at the contractor's convenience. The girders often camber upwards after initial stressing because of the eccentricity of the tendon profile. This camber then varies with time, as a function of the material properties, geometry and environment.

The uncertainty of the predicted camber in precast, prestressed girders can lead to problems during construction. Excessive camber leads to interference between the top of the girder and the deck reinforcement. Insufficient camber leads to an increase in the concrete required to meet the bottom of the deck slab, resulting in additional weight to the superstructure. Both are undesirable conditions that can lead to construction delays, as well as increased material and labor costs.

RESEARCH OBJECTIVES

The primary goal of this research was to improve the methods of predicting camber in precast, prestressed concrete girders. The research focused on evaluating current methods of predicting camber, collecting fabricator camber data to calibrate a model based on current methods, and implementing the methods. Specific objectives included the following:

- Evaluating current camber prediction methods.
- Developing a model to predict the camber history for a girder.
- Collecting girder design information and measured camber data for projects fabricated in Washington State.
- Evaluating the camber data collected in comparison with behavior predicted by current camber models.
- Providing recommendations to improve current camber prediction methods.

ANALYSIS PROCEDURE

A camber prediction program was developed to combine various methods of predicting compressive strength, elastic modulus, creep, shrinkage, prestress loss, and deflection. Several methods exist for modeling each characteristic. The program allows the user to select a set of methods and to apply them to the analysis on one or multiple girders.

The program considers the girder conditions in a series of time steps. At each step, the change in load, both due to changes in external load and changes in prestress, is treated as a new load case. The stresses and deformations caused by that load case are tracked separately as a function of time, and, at each time step, are added to those from each previous loading.

To begin a time history analysis of girder camber, the user must provide casting dates and times, shipping and placement times, girder geometry, concrete properties, and prestressing properties. The user then selects the desired method of calculation for each characteristic. For this research, the methods chosen were the ones recommended by the AASHTO LRFD, because they are the methods used by WSDOT.

The time series is customizable on the basis of the girders to be evaluated. Because the program calculates the prestress deflection on the basis of the incremental changes in prestress loss, it is best to use a time series with a fine time step. Although increasing the number of time steps increases the program run time, that increase in computational effort is only significant for large sets of girders.

The following sections describe the behaviors that most strongly affect camber. Elastic deflection and creep provide the two largest components of camber. Prestress loss is affected by both of these, and consequently, contributes indirectly to camber.

CONCRETE COMPRESSIVE STRENGTH AND ELASTIC MODULUS

The concrete compressive strengths at release and at 28-days are defined by the user. The program can use either the design strength or the actual measured strength of the concrete, and calculate the time history of the compressive strength based on the calibrated constants b and c in Equation 1¹.

$$f'_c(t) = f'_c(28) \frac{t_{str}}{b + ct_{str}} \quad (1)$$

where:

- t_{str} = time after concrete starts to gain strength
- b = constant that changes the rate of increase
- c = constant that changes the ultimate value
- $f'_c(28)$ = 28-day concrete compressive strength
- $f'_c(t)$ = concrete compressive strength

The elastic modulus of concrete is traditionally estimated on the basis of the concrete compressive strength. The AASHTO LRFD method for calculating the elastic modulus is shown in Equation 2².

$$E_c(t) = 33,000 K_1 w_c^{1.5} \sqrt{f'_c(t)} \quad (\text{ksi}) \quad (2)$$

where:

- K_1 = correction factor for source of aggregate (WSDOT uses $K_1 = 1.0$)
- w_c = unit weight of concrete (kcf)

CREEP AND SHRINKAGE

The factors affecting creep include volume-to-surface ratio, relative humidity and concrete strength. The AASHTO LRFD equation for creep not only provides a time-dependent relationship, but is also influenced by the age of the concrete at the time of loading, as shown in Equation 3². The creep coefficient is also defined as C_c .

$$\psi(t, t_a) = 1.9k_s k_{hc} k_f k_{td} t_a^{-0.118} \quad (3)$$

where:

- k_s = factor for the effect of volume-to-surface ratio
- k_{hc} = humidity factor for creep
- k_f = factor for the effect of concrete strength
- k_{td} = time development factor
- t_a = age of concrete at time of load application (day)

If the prestress were to remain constant while creep occurred, the camber would increase. However, the creep also leads to long term prestress loss, which reduces the camber. The net effect of creep on camber is the sum of these two processes.

Shrinkage of the girder, like creep, affects the camber both directly and through prestress loss. Its direct effect occurs only if the locations of the centroids of the steel and concrete differ, and even then it is very small. Girder shrinkage also contributes to prestress loss, which therefore reduces the camber. Differential shrinkage of the cast-in-place deck relative to the precast girder may have a significant influence on the camber because the centroids of the two elements are separated vertically by a considerable distance.

AASHTO LRFD estimates axial free shrinkage strain as a function of time and is used to provide the time dependence needed for predicting the prestress losses². The factors affecting shrinkage include volume-to-surface ratio, relative humidity and concrete strength as shown in Equation 4.

$$\varepsilon_{sh}(t) = -k_s k_{hs} k_f k_{td} 0.48 \times 10^{-3} \quad (4)$$

where:

- k_{hs} = humidity factor for shrinkage

The program uses a single value of surface/volume ratio for the girder, rather than subdividing it into sub-regions, such as flange and web. This approach is commonly used, but is not strictly correct, because it fails to predict any internal stresses and deformations in the girder due to different rates of shrinkage of the constituent parts.

PRESTRESS LOSSES

The total prestress losses are the cumulative result of many components and are important to predict because they can affect the observed camber in the prestressed member. The 2007 AASHTO LRFD Refined Method for estimating prestress losses estimates the amount of prestress loss in a girder by summing the losses from different components². Equation 5 shows that the losses are divided into two main categories: instantaneous losses and time dependent losses.

$$\Delta f_{pT} = \Delta f_{pES} + \Delta f_{pLT} \quad (5)$$

where:

Δf_{pES} = sum of all losses or gains due to elastic shortening or extension at the time of application of prestress and/or external loads (ksi)

Δf_{pLT} = losses due to long-term shrinkage and creep of the concrete, and relaxation of the steel (ksi)

$$\Delta f_{pLT} = (\Delta f_{pSR} + \Delta f_{pCR} + \Delta f_{pR1})_{id} + (\Delta f_{pSD} + \Delta f_{pCD} + \Delta f_{pR2} + \Delta f_{pSS})_{df} \quad (6)$$

Each time dependent component is estimated during two time regimes. These are defined as the time between release of the prestressing and deck casting and the time between deck casting and a final time.

CAMBER CALCULATIONS

Camber (at midspan) is calculated by summing the deflections caused by individual loadings, including self-weight, prestress, and additional dead loads. Camber is defined as positive upwards.

Self-Weight Deflection

Self-weight deflection is calculated by using a uniformly distributed load over the length of the girder. Because, during storage and transportation, the supports of the girder are typically not located at the ends, the equation for a simply supported beam does not apply. Therefore, Equation 7 is used to calculate the total camber from the end of the girder to the midspan².

$$\Delta_{SW} = \Delta_{MIDSPAN} - \Delta_{OVERHANG} \quad (7)$$

where:

$\Delta_{MIDSPAN}$ = the deflection at midspan relative to the support

$$= \frac{\omega_{sw} L_n^2}{384 E_c I_g} [5L_n^2 - 24L_c^2] \quad (8)$$

$$\begin{aligned} \Delta_{OVERHANG} &= \text{the deflection of the overhang relative to the support} \\ &= \frac{\omega_{sw} L_c}{24 E_c I_g} [3 L_c^2 (L_c + 2 L_n) - L_n^3] \end{aligned} \tag{9}$$

L_c = length of girder overhang
 L_n = length of girder span between supports

For a girder of total length L , supported on rollers a distance αL from each end, Equation 7 can be expressed as

$$\Delta_{MIDSPAN} = \Delta_0 f(\alpha) \tag{10}$$

where:

$$\Delta_0 = \frac{5 w_{sw} L^4}{384 E_c I_g}, \text{ and} \tag{11}$$

$$f(\alpha) = (1 - 2\alpha)^2 (1 - 4\alpha - 0.8\alpha^2) \tag{12}$$

The function $f(\alpha)$, is plotted against α in Figure 1.

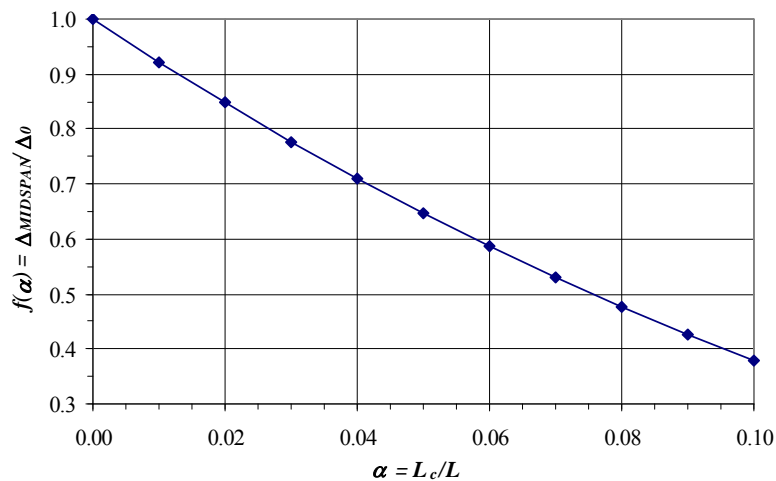


Figure 1 Effect of Overhang on Girder Deflection

The initial slope of the curve is -8, so an overhang of 1% of the total length causes the mid-span deflection due to self weight to be multiplied by a factor of approximately $(1 - 8 * 0.01) = 0.92$ compared with the value for a girder of the same total length supported at its ends. The overhang reduces the mid-span deflection in two ways; it shortens the central span, thereby reducing the deflection, and it causes an end moment, which further reduces the mid-span deflection.

Prestressing Deflection

The deflection due to the prestress force is given by Equation 13. The effective eccentricity is used at the end and midspan to include all the strands that contribute to that deflection component.

$$\Delta_{ps} = \frac{PL^2}{8E_c I_g} \left[e_{mid} + (e_{end} - e_{mid}) \frac{4a^2}{3L^2} \right] \tag{13}$$

WSDOT PRACTICE FOR CAMBER PREDICTION

Until recently, the AASHTO LRFD Bridge Design Specifications 2004 edition was used for the WSDOT Bridge Design Manual⁴. However, the 2007 Edition was adopted recently.

PGSuper is a design and analysis program for the AASHTO LRFD Bridge Design Specifications and is a product of the WSDOT Bridge and Structures Office³. PGSuper uses the AASHTO methods described in this chapter to calculate the effects of shrinkage and creep and to estimate deflection. The camber model shown in Figure 2 illustrates the components of camber that WSDOT calculates to approximate the camber changes during the life of a girder³.

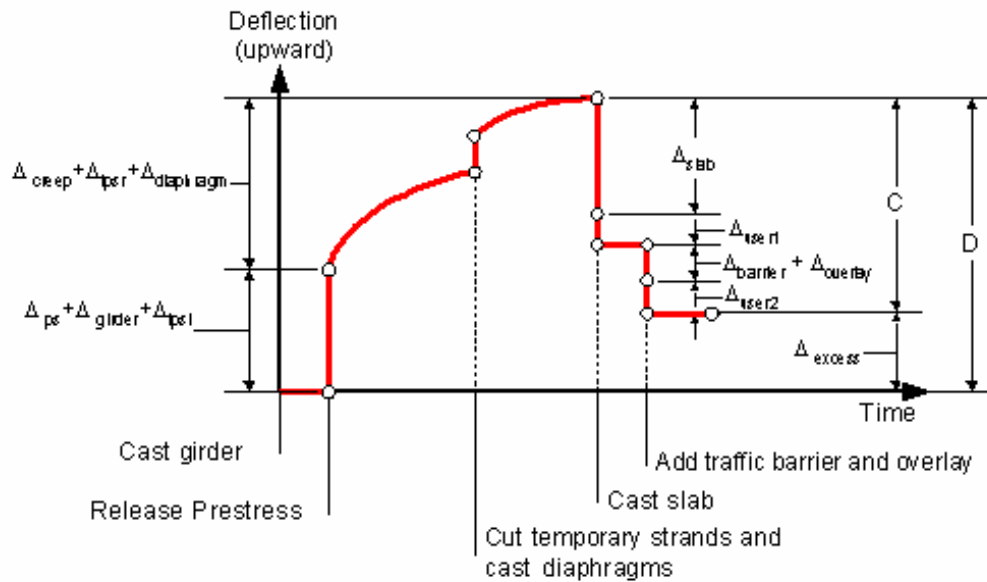


Figure 2 WSDOT Camber History Model³

While Figure 2 is helpful to establish the chronology of events, WSDOT does not typically develop a full time history of camber for a girder. Instead, earliest and latest times are given for critical events.

The creep deflection is calculated by multiplying the creep coefficients by the corresponding elastic deflections (i.e. self-weight, permanent strands, temporary strands). Time dependent changes in prestress are not considered in the prestress deflection at any time after release.

PGSuper also makes several important assumptions. The design length of the girder is defined as the length from the centerline of the final bearing at both ends. All deflection calculations are based on the span length using a simply supported model. PGSuper also assumes that once the deck has been cast, the stiffness of the superstructure increases because of the composite action. The effects of creep will therefore become insignificant and are ignored. However, by then, the camber of the girders is generally not considered to be a problem.

MATERIALS DATA

During this research, eight girders were cast at Concrete Technology Corporation (CTC) for the Snake Lake Bridge project. They were used as an opportunity to obtain detailed camber records over the first two months of the girders' lives and to obtain corresponding materials data that could be used for comparing the girder behavior with that predicted from the materials data. Material tests were performed on concrete from six of the girders to evaluate the compressive strength, elastic modulus, shrinkage, and creep properties. Testing was typically performed at the approximate time of release and at multiple subsequent times. The exact number of tests depended on the number of cylinders available. The girders were constructed using one of three different mixes (numbers 130, 140 and 190), according to the release strength requirements. The mixes were very similar to each other. Most cylinders received accelerated curing, using the same temperature program as for the girder. This is CTC's standard practice. Some moist-cured cylinders were also prepared.

CONCRETE COMPRESSIVE STRENGTH TEST RESULTS

Compressive strength tests were performed on the concrete to observe the relationship between strength and maturity. Figure 3 shows the results of the University of Washington (UW) and CTC concrete compressive strength tests for the accelerated-cured and moist-cured cylinders.

To better model the behavior of the specific mix, the "best fit" coefficients were found by minimizing the error between the measured values and those predicted and by Equation 1. The fit was achieved by varying the constants b , c and t_{str} . Still, the model did not predict well the concrete compressive strength of the accelerated-cured cylinders for the tests that were performed between two and ten days. The difficulty in fitting the data throughout the 28-day period may have been a consequence of the fact that the cylinders were subjected to two curing environments (heated before release and ambient afterwards).

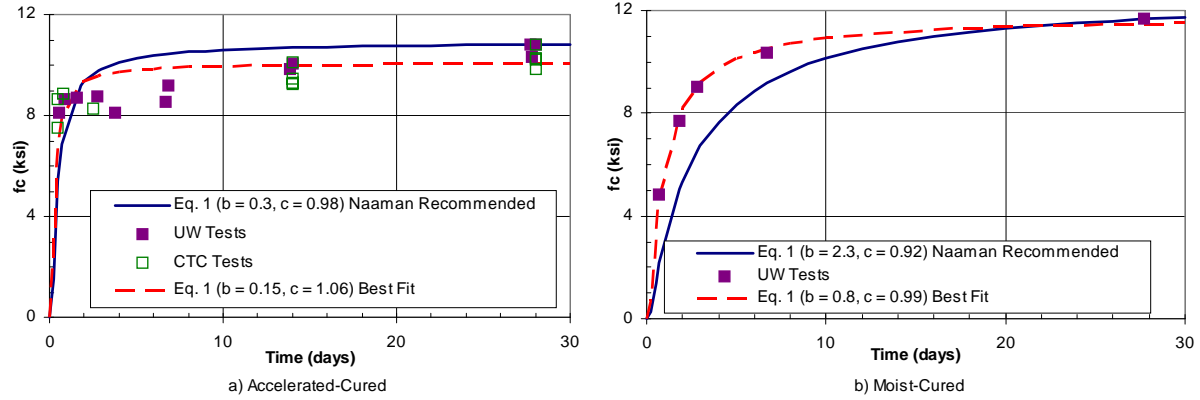


Figure 3 Snake Lake Bridge Project Concrete Compressive Strengths a) Accelerated-Cured Cylinders b) Moist-Cured Cylinders

ELASTIC MODULUS TEST RESULTS

An elastic modulus test was conducted to correspond with each compressive strength test. To obtain data for additional times, some supplemental elastic modulus tests were performed on cylinders that were later used for the 28-day compressive strength test. All elastic modulus tests were conducted on accelerated-cured cylinders except for several tests on the cylinders from one girder (G1D).

Figure 4 plots the elastic modulus test values against the age of the concrete cylinders and the concrete compressive strength.

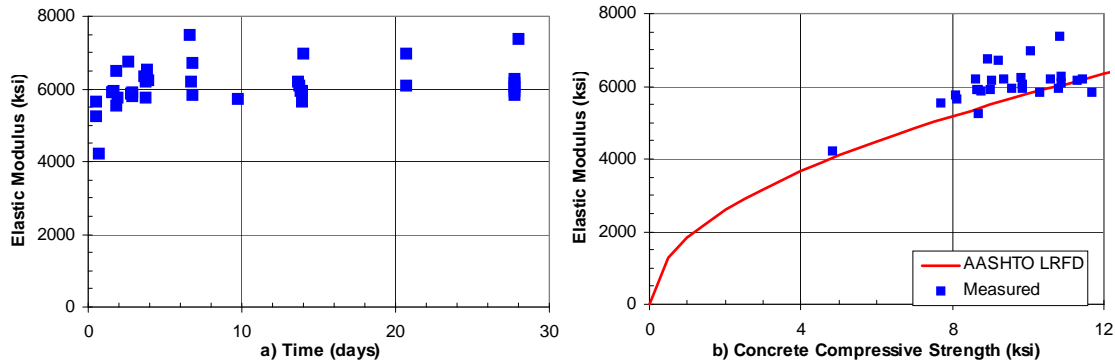


Figure 4 Snake Lake Bridge Elastic Modulus Test Results a) vs. Time b) vs. Concrete Compressive Strength

During the first few days, the elastic modulus tended to increase with increasing age. The moist-cured (MC) cylinders for Girder G1D of mix #130 had a smaller elastic modulus value at release, as would be expected because of that girder’s lower concrete compressive strength at release. However, as the moist-cured cylinders matured, the elastic modulus of these cylinders approached that of the accelerated-cured cylinders. On average, the measured

elastic modulus was 8 percent higher than the value predicted by the AASHTO LRFD method.

SHRINKAGE AND CREEP TEST RESULTS

Shrinkage and creep tests were performed on accelerated and moist-cured cylinders. These tests were performed on the concrete mix that was used for the Snake Lake Bridge project girder G1D, mix #130. Eight stacks consisting of two cylinders each were prepared. Moist-cured cylinders were used for four of the stacks, and accelerated cured-cylinders were used for the remaining four. One stack of each cure type was loaded after one day of curing (same time as release of prestress), three days of curing, and seven days of curing. The remaining stacks (one of each cure type) were not loaded but were monitored to determine the effects of shrinkage. Each stack included a short steel cylinder between the two concrete ones. This was necessary because the available mechanical strain gage had a 10 in. gage length, but the individual cylinders were only 8 in. long.

Shrinkage

The observed behaviors of the accelerated-cured and moist-cured shrinkage specimens were surprising. Only the unsealed, moist-cured cylinder consistently shortened with cylinder age (i.e., negative strain). The other cylinders elongated or changed little in length. This elongation was not expected. Individual data points may have been affected by the difficulties that were experienced with the measuring equipment, but the overall trend is believed to be real. This view is supported by the results of a follow-up study⁵ on different batches of the same concrete mix designs. That study used a larger number of specimens and new measuring equipment. No difficulties were found with the measurement techniques but the results found the same trends as were observed here.

Creep

Creep tests monitored the cylinder strain over time after the initial load had been applied. Figure 5 shows the creep rig assembly used for one stack. The central steel cylinder can be seen between the unsealed lower cylinder and the upper one sealed with adhesive foil furnace tape.



Figure 5 Creep Rig Assembly

Figure 6 shows the total change in concrete strain for the accelerated-cured and moist-cured cylinders. Each cylinder was designated by the age of the cylinder at loading and whether it was sealed or unsealed. The strain results shown include strain changes due to shrinkage and are considered the total strain.

The sealed and unsealed cylinders were intended to simulate large (sealed) and small (unsealed) volume-to-surface ratios. For both the accelerated-cured and moist-cured cylinders, the unsealed cylinders crept more than the cylinders that were sealed. This difference is likely attributable to the drying shrinkage and creep that occurred in the unsealed cylinder while the sealed cylinders retained their moisture.

The moist-cured cylinders showed a wider range in strain with respect to the age of loading and sealing conditions. However, the sealed moist-cured cylinders displayed lower concrete strains than the sealed accelerated-cured cylinders because their strengths were lower, and lower loads were therefore applied. If the sealed cylinders were assumed to be completely devoid of shrinkage strain due to loss of free water, then differences between the two might be attributed to different quantities of creep strain or different quantities of shrinkage strain due to chemical hydration.

The global trend of the results was as expected. With time, the concrete strain increased but it did so at a continually decreasing rate.

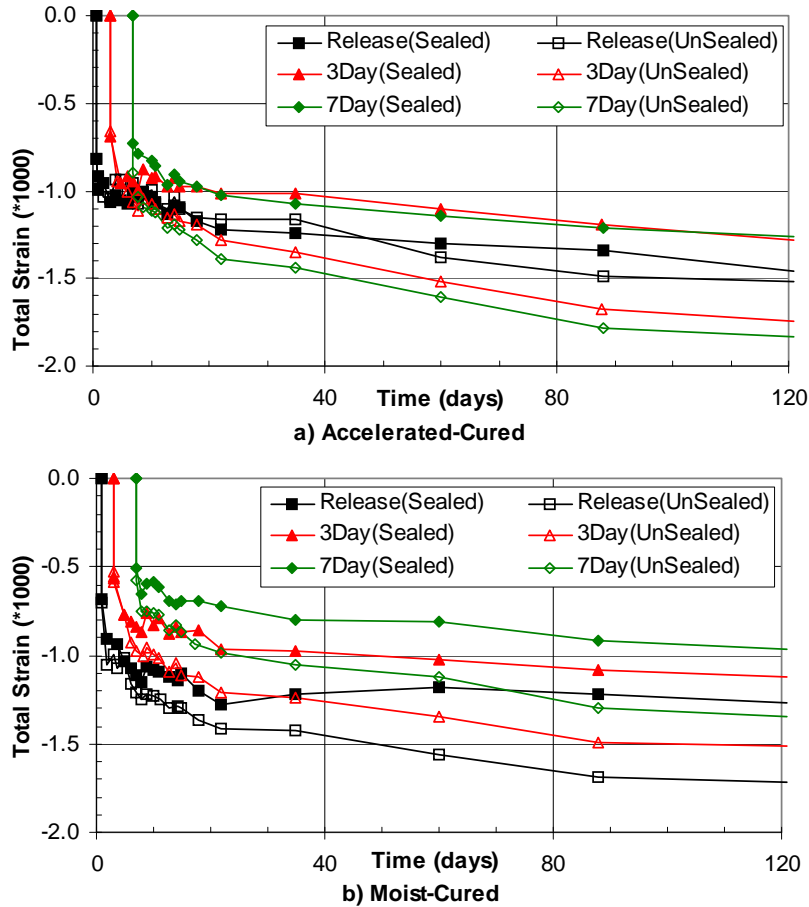


Figure 6 Snake Lake Bridge Girder G1D Strain History
a) Accelerated-Cured, b) Moist-Cured

DETAILED IN-PLANT DATA COLLECTION

A detailed camber history study was conducted on eight girders from the Snake Lake Bridge project at CTC’s fabrication yard in Tacoma. All of the girders had W74G sections and were 135 feet long. The numbers of straight and temporary strands were the same for all the girders: 26 and 6, respectively. However, the number of harped stands varied from 11 to 18. This variation was a result of the placement location of each girder on a two-span bridge widening project. The “A” and “D” in the mark number indicate the span, while the G1 and G4 girders were exterior, and the G2 and G3 girders were interior, adjacent to the existing superstructure.

Girders G1A and G2D were cast on Fridays and are denoted as “weekend” girders. However, G1A matured over the Labor Day weekend, resulting in 3.5 days of curing before release. The remaining girders were cast and released in less than one day except for G4D. For this

girder, the required release strength was not reached after one day of accelerated curing, so the prestress release was delayed until the second day.

After the prestress had been released, the girder was moved to the finishing yard and placed on timber supports. A camber reading was then taken by the University of Washington (UW) researchers on both faces of the girder. After girder camber had been measured on both sides of the girder, gross errors in measurement could be detected by comparing the readings from the two sides. Camber readings were taken daily after release to monitor the early effects of creep. The measurements were then taken at longer intervals as the rate of camber change decreased. In order to minimize the effects of thermal gradient, camber readings were always taken in the early morning. Furthermore, the monitoring occurred during September and October, when intense solar radiation is unusual in Western Washington, even at mid-day.

All of the girders showed an increase in camber during the duration monitored. Figure 7 shows the camber measurements recorded for all eight girders.

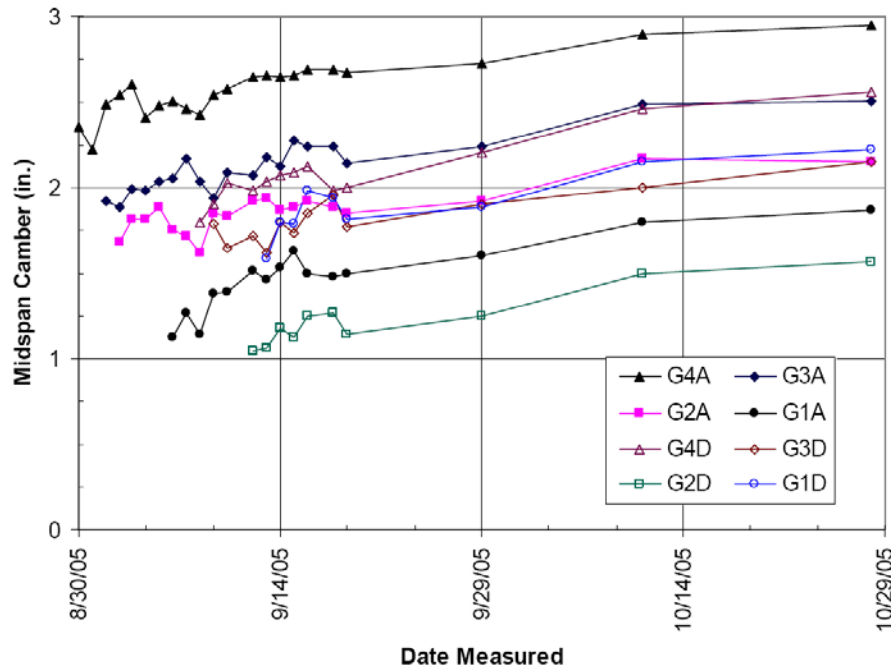


Figure 7 Snake Lake Bridge Girders – Measured Camber Data

The camber history did not produce smooth curves. Possible causes for the variations in the curve might include measurement inaccuracy and thermal gradient. The measurements were taken with a laser level and a special rod that was designed to register accurately on the bottom flange of the girder. Measurements taken by a single operator were found to be repeatable to better than 1/8 in. However, it is possible that differences occurred between operators. The temperature over the height of the girder was checked and found to be on the

order of one or two degrees F. The corresponding thermally-induced camber is less than 1/8 in

FIELD DATA

The two largest fabricators of prestressed concrete girders in the state of Washington are Concrete Technology Corporation (CTC), located in Tacoma, and Central Pre-Mix Prestress (CPM), based in Spokane with an additional prestressing plant in Pasco. Girder cambers were collected from the fabricator’s quality control record and field measurements on the Keys Road Bridge project.

FABRICATOR DATA

To obtain data on a broad range of girders used in WSDOT bridges, site visits were made to those two companies, and data were collected from a total of 146 girders. Because of the range in size and length of the girders used in WSDOT bridges, an effort was made to collect data that varied in cross-section, length, and the amount of prestressing used. The information gathered from quality control records and fabrication shop drawings included camber measurements at release and at one subsequent time, girder geometry, material data, level of prestressing, and curing information. Figure 8 shows the population distribution for girder length and section type. Data for 103 girders were collected from Concrete Technology Co. and for 43 girders from Central Pre-Mix.

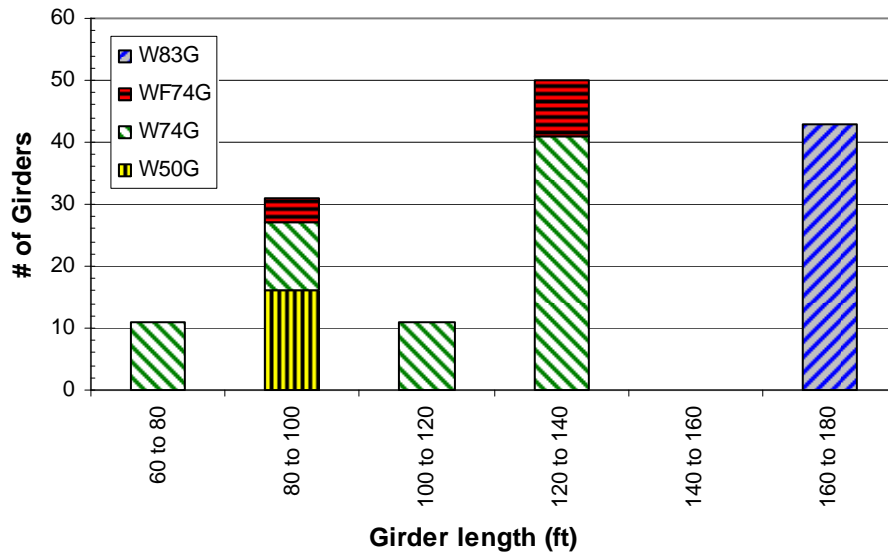


Figure 8 Number of Girders for Each Section

Additional variations targeted in the data collection included differences in the age of concrete at release and seasonal variations during casting. Figure 9 shows the number of girders collected for each section type, fabricator and the bridge project.

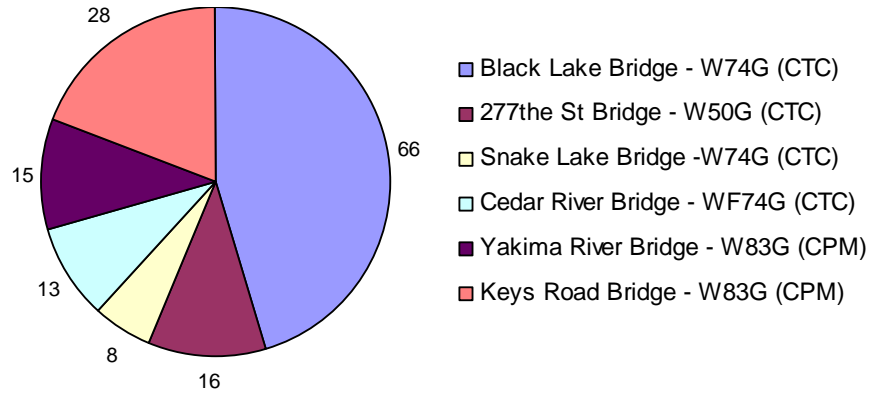


Figure 9 Number of Girders by Project, Section, and Fabricator

Effects of Concrete Maturity at Release

The elastic modulus at release is not routinely measured, so it usually has to be inferred from strength data using relationships such as those proposed by ACI 318, AASHTO, ACI 363, and others. If detailed records of strength versus time are not available, approximate relationships between strength and maturity may be used to estimate strength gain with time.

Figure 10 shows measured strengths and release cambers versus the maturities from the 277th St Bridge, Cedar River Bridge, and Black Lake Bridge projects.

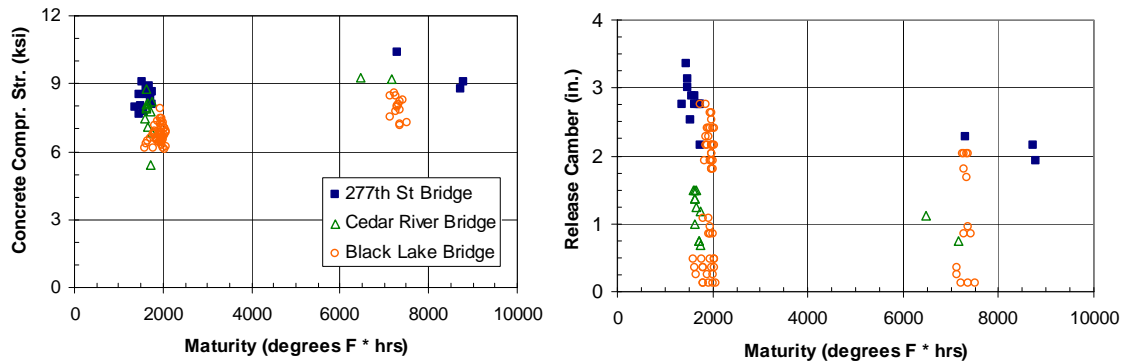


Figure 10 Effects of Maturity at Release

The figure shows that the concrete gained strength as it matured by curing over a weekend or holiday. Because the heat of hydration raised the temperature above ambient for an extended time, the fabricator was able to reduce energy consumption by turning off the external heat earlier than usual while still maintaining the maturity required to achieve the desired strength. Despite the early cut-off of external heat, the maturities were much higher and the strengths were slightly higher (on average 15 percent) than those of the girders released after one day. As the maturity increased, the concrete strength increased, the girder became stiffer and the

release camber dropped. A large increase in maturity beyond that achieved in the first sixteen hours of curing led to only a small increase in strength.

Influence of Compressive Strength on Release and Long Term Camber

The compressive strength at release and 28 days can influence the release camber by changing the stiffness of the girder. The Black Lake Bridge project had smaller cambers at release when the release concrete strength was higher. However, this trend was not observed in the girders with low cambers. This may be attributable to measurement errors, which become more important for small cambers.

The long-term trends were more difficult to distinguish. The longer spans of 126 ft and 132 ft showed a weak trend of lower long-term cambers with higher strength. This tendency is rational, in that the higher strength implies higher elastic modulus and lower creep coefficient. The long-span data also showed that the girders released after more than one day exhibited less long-term camber than girders released at less than one day.

KEYS ROAD FIELD DATA

The camber monitoring data for the Snake Lake girders did not show effects of the release of temporary strands and deck placement. To evaluate the effects of these operations further, a detailed camber study was conducted on 91 girders for the Keys Road Bridge project. The girders were cast in Pasco, Washington, by the Central Premix Prestress Co. (CPM) and shipped to the project site in Yakima, Washington. Cambers were measured before and after the release of the temporary strands; before and after the cast-in-place deck pour; and at monthly intervals after these events. As many as nine and as few as four sets of camber measurements were taken on each of seven spans from November 30, 2005, to November 13, 2006.

All of the girders measured had W83G sections and were approximately 178-ft long. The bridge had nine spans of 13 girders each. Spans 1 and 2 were inaccessible and not monitored. The middle seven girders of each span are referred to as the interior girders, whereas the three on each side of the span are referred to as the exterior girders. The girder schedule in the contract plans shows that the amounts of prestressing steel and the concrete strengths differed slightly between these two types of girders.

The end conditions varied among the spans as shown in Figure 11. In spans 4, 5, 6, and 8 the construction procedure caused the piers to provide some restraint to the girder end rotation. Therefore, those spans behaved as partially restrained at both ends. Specifically, the girders in them were placed on oak blocks, braced laterally, and the temporary strands were released. The bottom flange was then embedded 7 in. into the pier, with an 18-in.-deep concrete step covering the bottom flange. The diaphragms were cast, the deck was placed, and the pier closure pour was cast. In each of the remaining spans (3, 7, and 9), one end of the girder was cast continuously, as described above, and the other end was placed on an elastomeric bearing pad to allow some rotation and displacement.

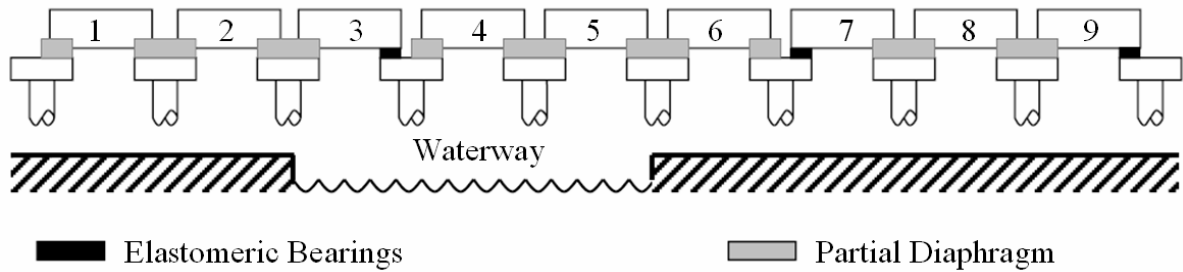


Figure 11 Keys Road Bridge – Support Conditions for All Spans

Table 1 provides statistics on the accuracy of the calculated cambers. The table separates the interior and exterior girders and considers the calculated values by using both the design and measured concrete compressive strengths. The calculated deflections for actual concrete compressive strength also included the 15 percent increase in elastic modulus, as recommended in the Calibration of Analytical Model section, presented later in the paper. The mean and standard deviations were calculated by using all of the girders in the defined set of measured deflections. All deflections were calculated by assuming the girders to be simply supported.

Table 1 Measured and Calculated Changes in Camber

		$(\mu \pm \sigma)$	2 Ends Continuous		1 End Continuous	
			Exterior	Interior	Exterior	Interior
Temporary Strands Rel.	Δ_m (in.)		0.76 ± 0.16	0.73 ± 0.19	1.05 ± 0.28	1.05 ± 0.27
	$\Delta_m/\Delta_c(\text{Design } f'_c)$		0.70 ± 0.15	0.68 ± 0.18	0.98 ± 0.26	0.98 ± 0.25
	$\Delta_m/\Delta_c(\text{Actual } f'_c)$		0.88 ± 0.19	0.84 ± 0.22	1.22 ± 0.31	1.21 ± 0.29
Deck Placement	$\Delta_m (\mu \pm \sigma)$ (in.)		-1.54 ± 0.41	-1.13 ± 0.47	-1.79 ± 0.81	-1.96 ± 0.64
	$\Delta_m/\Delta_c(\text{Design } f'_c)$		0.57 ± 0.15	0.41 ± 0.17	0.66 ± 0.32	0.72 ± 0.25
	$\Delta_m/\Delta_c(\text{Actual } f'_c)$		0.71 ± 0.20	0.51 ± 0.21	0.82 ± 0.39	0.90 ± 0.56
Deck Creep*	$\Delta_m (\mu \pm \sigma)$ (in.)		-0.46 ± 0.70	-0.40 ± 0.70	-0.46 ± 0.49	-0.32 ± 0.56
	$\Delta_m/\Delta_c(\text{Design } f'_c)$		0.40 ± 0.63	0.35 ± 0.62	0.42 ± 0.44	0.29 ± 0.51
	$\Delta_m/\Delta_c(\text{Actual } f'_c)$		0.53 ± 0.86	0.45 ± 0.81	0.54 ± 0.56	0.36 ± 0.56
Deck Creep**	$\Delta_m (\mu \pm \sigma)$ (in.)		-0.46 ± 0.70	-0.40 ± 0.70	-0.46 ± 0.49	-0.32 ± 0.56
	$\Delta_m/\Delta_c(\text{Design } f'_c)$		0.72 ± 1.11	0.62 ± 1.11	0.74 ± 0.78	0.51 ± 0.90
	$\Delta_m/\Delta_c(\text{Actual } f'_c)$		0.94 ± 1.52	0.79 ± 1.43	0.95 ± 0.99	0.64 ± 1.16

m = measured, c = calculated

* Using girder section properties only.

** Using composite section properties ($1.77 \cdot I_g$).

Effect of Actual Concrete Strength

The accuracy increased and the calculated cambers decreased significantly when the actual (rather than the design) concrete strength was used. This trend was expected because the actual stiffness of the concrete was greater than the value assumed in design. On average, the measured concrete strength at release exceeded the design strength by 11 percent. The measured strength at 28 days exceeded the design strength by an average of 17 percent.

Camber Changes at Release of Temporary Strands

The release of temporary strands provides an opportunity to evaluate the effects of some of the parameters that might influence the response, such as interior versus exterior girder and the end restraint provided by the support conditions. The response of the exterior and interior girders to strand release was nearly identical. Both types of girder had the same number of temporary strands and, at the time of monitoring, the deck had not yet been cast, so they were expected to behave similarly. The accuracy of the camber predictions for both types was therefore also similar.

By contrast, the end restraint had a significant effect on the measured cambers. The camber change in the spans with two ends continuous was only 71 percent of that in the spans with one end continuous. This finding suggests that the oak blocks produced significant end restraint, rendering the span 41 percent stiffer than a truly simply supported one.

In the spans with one end continuous, the measured camber changes were significantly (21 percent) larger than the values calculated with the actual concrete strength and unrestrained supports. This result was unexpected, because any additional effects that are not accounted for in the calculations are likely to provide restraint, rather than adding flexibility, and would therefore stiffen the system and reduce the camber change. The only exception is cracking. However, the load on the girders prior to release of temporary strands is so small that cracking is most improbable. Therefore, the results are regarded as anomalous, and the reasons for them remain unknown.

Camber Changes Due to Casting of the Deck

On average, when the deck was cast the spans with two ends restrained were 46 percent stiffer than those with only one end restrained. (The interior and exterior girder showed rather different deflection ratios of 1.155 and 1.764 respectively, but the average was 1.46). This may be compared with the 41 percent additional stiffness observed for the temporary strand release. At strand release, only oak blocks restrained girder end movement, whereas at deck casting the pier cap embedment was also in place. The similarity in stiffness increase suggests that both systems prevented relative displacement between the girder and pier cap almost completely, and that almost all of the flexibility present was provided by deformations of the piers, which are assumed to have been the same on both occasions.

Some inconsistencies are apparent in the measured data, but they may have been caused by the relatively large scatter in the cambers for different girders. The average coefficient of variation was 36 percent.

Camber Changes after Deck Placement

The deflection measurements after the deck placement had significant amounts of scatter, with an average coefficient of variation of 152 percent. Approximately 0.4 in. of additional deflection (downward) was observed on average over the monitored time period for all the girders, while the standard deviation was as high as 0.70 in. This relatively large scatter is attributed to the fact that the creep deflections were quite small (relative to the initial camber) and that the deflections due to other loadings, such as thermal effects, differential shrinkage and changes in construction loading, were not considered but were undoubtedly present.

Span 8 girders consistently deflected upwards, whereas spans 6, 7, and 9 all deflected downwards. The reason for the difference remains unknown. Spans 3, 4, and 5 lay over the waterway, and deflections readings could not be taken for them after the deck pour.

The calculated creep deflection was initially based on the elastic deck placement deflection, which was computed with the properties of the bare girder. To include the influence of the deck properly would require a time history of the compressive strength, elastic modulus, shrinkage and creep of the deck concrete, but these data were not available. Therefore, differential shrinkage was ignored and an upper bound on the time-dependent deflection was obtained by multiplying the elastic deflection by the creep coefficient. On average, the measured time-dependent camber change was only half of that computed with the actual concrete strength and the bare girder section. Thus, use of the composite inertia led to a better estimate of the time-dependent camber change (see Table 1).

END RESTRAINT FROM TEMPORARY SUPPORTS

The camber of a girder may be restrained by the build-up of axial force when the support restrains shrinkage and creep. The horizontal force acts at the bottom flange level, which induces an end moment that leads to downward deflection. Release of those forces by lifting the girder might be expected to cause the restrained camber to rebound. Tests were conducted to observe the magnitude of the camber rebound in a girder when one end was lifted off its support and placed on a steel roller between two plates.

All five of the girders tested were from the Key Road Bridge project. They were W83G sections, 178 ft long and placed on timber bunks located approximately 20 and 30 in. from the girder ends. The bunks were approximately 12-in. by 12-in. in cross-section and lay directly on the ground. The soil was a loosely compacted mixture of gravel and sand, which might allow for rotation of the support if the girder were to shrink.

Before lifting, the camber of each girder was measured on both sides. One end of the girder was then lifted at the lifting loop by the traveling crane and was set down again on the roller.

The camber was measured on each side of the girder and compared to the values obtained before lifting.

The midspan camber for all five girders increased after they had been placed on the rollers. Figure 12 shows the camber changes. The average increase was 0.165 inches. The consistent increase in camber suggests that the supports had been restraining some girder shortening due to creep and shrinkage.

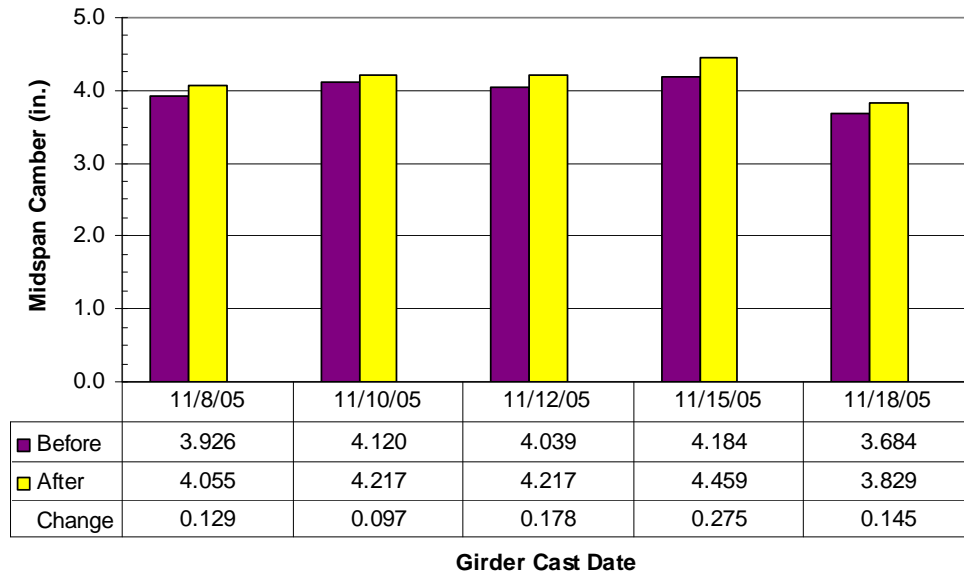


Figure 12 Roller Test Camber Results

When girders are shipped, any stresses caused by shrinkage restraint are released. The camber after shipping and erection should therefore be expected to be larger than that in storage. The final camber is of interest. Any method for predicting final camber that is calibrated with data that do not account for the effects of shrinkage restraint in the storage area is therefore likely to contain this modest error.

CALIBRATION OF ANALYTICAL MODEL

The calibration of the analytical model included multiple steps that started with the current procedure for predicting camber. Next, the model was changed to include the actual concrete strengths at release and at 28-days. Prestress losses were included in the time-dependent deflection calculations, and finally factors were applied to the elastic modulus and creep coefficient to minimize the predicted error.

The error is defined as the measured value minus the predicted one. Thus a negative error indicates that the predicted upward camber is larger than the measured, and that the real girder is flatter than the calculations suggest.

EVALUATION OF CURRENT PROCEDURE

In the first phase of this project, the WSDOT prediction method was evaluated for prestress losses according to the AASHTO LRFD 2004 provisions because that was the method WSDOT used at the time. WSDOT has since adopted the 2007 edition of the AASHTO LRFD, and the new equations for prestress losses resulted in better camber results. The major contribution was the reduction in losses due to creep deflection. Therefore the use of the 2007 AASHTO equations is considered the current WSDOT method for prediction.

Figure 13 shows the camber error of the calculated values using the design concrete compressive strength compared with the measured cambers at release and at a later time using the current WSDOT practice. The WSDOT method over-predicted the camber in almost all girders shown that were over 100 feet long. The range of error also varied for each project and length.

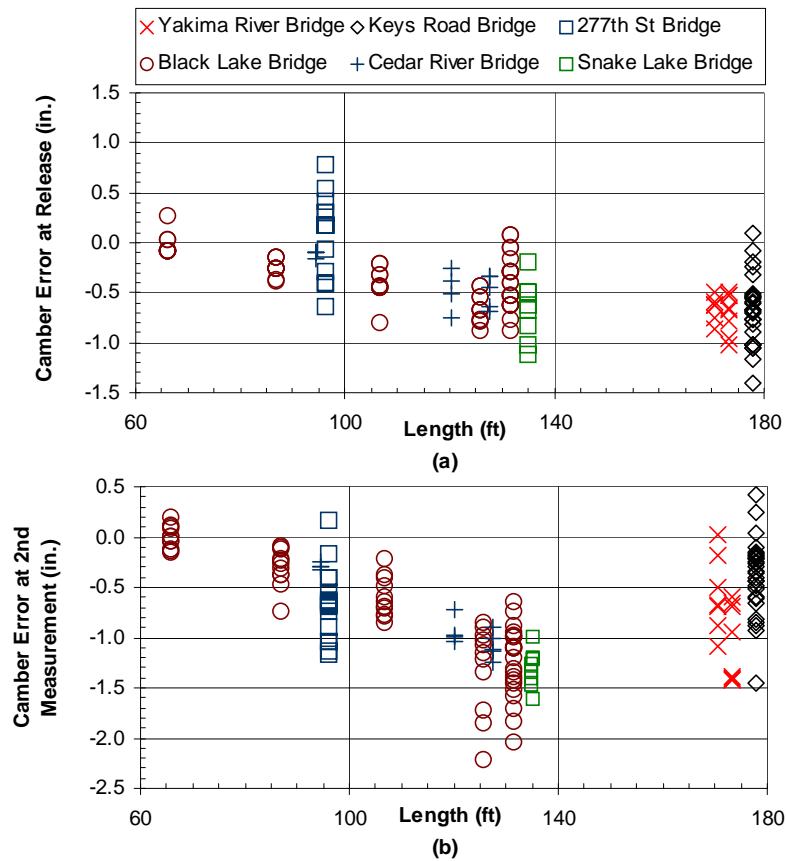


Figure 13 Camber Prediction Error Using the WSDOT Method a) At Release b) At Second Measurement

EFFECT OF USING MEASURED CONCRETE COMPRESSIVE STRENGTH

In general, the highest concrete stress occurs at release, so those conditions control the concrete mix design, and the specified 28-day compressive strength is often exceeded. Consequently, the girder tends to be stiffer and deflect less than would be the case if the actual strength had been based on the long-term requirements. On average, the actual concrete strengths at release and at 28 days exceeded the design values by 11% and 24%, respectively.

PRESTRESS LOSS DEFLECTION ADJUSTMENT

Creep in the concrete affects the magnitude of the prestressing force over time, and thus the camber due to prestressing, in two ways. First, if the prestressing force were to remain constant, creep of the concrete would increase the camber because the effective modulus of the concrete would decrease. This effect is taken into account as the “creep deflection” in the WSDOT method. However, creep also causes a gradual reduction in prestress force over time. This, in turn, causes a reduction in camber due to prestressing, including both the elastic and creep components. The second effect represents an interaction between the prestressing and creep effects and is not accounted for in the WSDOT method, which therefore over-estimates the camber due to prestressing.

CALIBRATION OF CAMBER PREDICTION MODEL

Further improvements in camber prediction, beyond those available from incorporating the two foregoing effects, were sought. They were achieved by applying factors to two of the components of the camber and optimizing their values to minimize the camber error. Modification factors were applied to the elastic deflection caused by the self-weight and the release of the prestressing strands, and the additional deflection due to creep.

A modification factor on the prestress losses due to creep was also considered. However, the modification did not significantly reduce the calculated error. Therefore, the researchers decided to use the least possible change to the prestress loss because that behavior had been subjected to extensive recent study⁶ and should be regarded as reliable.

Predicted creep deflection is affected by the elastic modulus, but the converse is not true. Therefore the calibration was conducted in steps, the first of which was to determine the elastic modulus from the (elastic) release cambers. Then the elastic modulus was held constant while the creep coefficient was adjusted to achieve the best fit between predicted and measured camber at the second camber measurement.

Calibration of Elastic Modulus

The procedure involved selecting a value for the elastic modulus modification factor and computing the predicted release camber for all the girders. In this process, the prestress losses due to relaxation before transfer and elastic shortening were computed according to the

AASHTO LRFD 2007 method. Figure 14 shows the calibration for the elastic modulus for all the girders, girders fabricated at CTC, and girders fabricated at CPM.

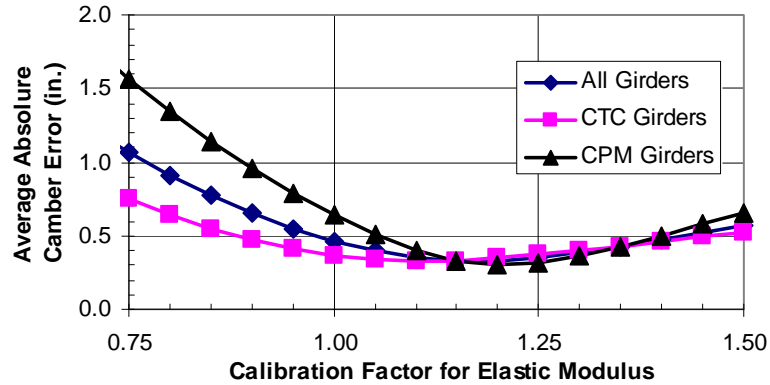


Figure 14 Calibration of Elastic Modulus at Release

The factors that minimized the average elastic deflection error at release were 1.15 for all girders, 1.10 for CTC girders, and 1.20 for CPM girders. The difference is attributed to the fact that the two companies are located in different parts of the state and use different aggregates.

Calibration of Creep Coefficient

Using the calibrated elastic modulus from the release camber measurement, the creep coefficient, C_c , was calibrated to minimize the average absolute camber error for the second camber measurement. An infinite number of combinations of factors for the elastic modulus and creep coefficient existed to minimize the average error. Each combination was about as good as the next. This observation allows the factors for elastic modulus and creep to be established independently. Therefore, the elastic modulus factor selected was accepted, and the creep coefficient factor was chosen as 1.4 minimizing the average absolute camber error.

Figure 15 shows the predicted camber error for all the girders using all the adjustments previously described: actual concrete compressive strength, inclusion of prestress losses in deflection calculation, elastic modulus factor of 1.15, and creep coefficient factor of 1.4.

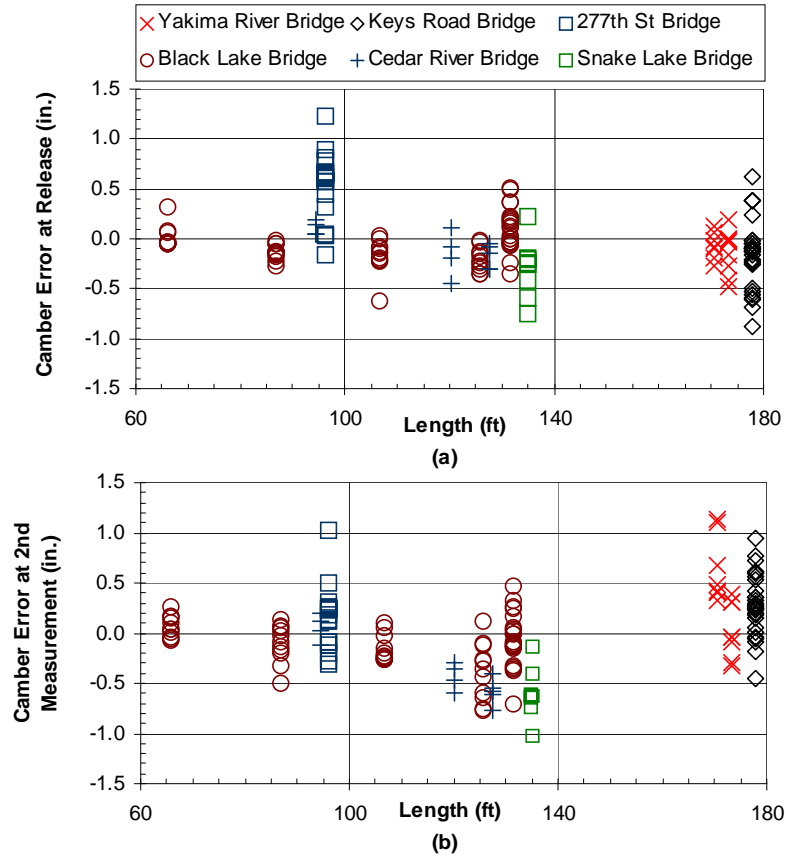


Figure 15 Camber prediction Error Resulting from the Use of the Modified Elastic Modulus and Creep Coefficient (E_c Factor = 1.15, C_c Factor = 1.4) a) At Release b) At Second Measurement

DISCUSSION

Table 2 shows the change in error resulting from the introduction of each modification procedure. The largest reduction in error occurred when all the modification procedures were used together. In addition, the basic WSDOT method using the design concrete compressive strength was replaced by the modified method with all the modification factors and the actual concrete compressive strength.

Table 2 Reduction in Errors Resulting from the Use of Various Predictive Methods

Percent Error Reduction for Method Comparisons	Release Measurement (in.)			2nd Measurement (in.)		
	Average Error	Average Absolute Error	Standard Deviation	Average Error	Average Absolute Error	Standard Deviation
WSDOT (DCS) to WSDOT (ACS)						
All	-30%	-19%	-2%	-43%	-39%	-25%
CTC	-43%	-22%	-6%	-49%	-45%	-29%
CPM	-17%	-16%	6%	-24%	-17%	-5%
WSDOT (ACS) to Modified WSDOT (ACS)						
All	0%	0%	0%	-104%	-35%	-1%
CTC	0%	0%	0%	-75%	-39%	-10%
CPM	0%	0%	0%	-172%	-25%	-18%
Modified WSDOT (ACS) to Mod. WSDOT w/ Factors (ACS)						
All	-90%	-37%	-8%	-180%	2%	1%
CTC	-110%	-92%	4%	-36%	-6%	-3%
CPM	-76%	-57%	-1%	-78%	-19%	6%
WSDOT (DCS) to Mod. WSDOT w/ Factors (ACS)						
All	-93%	-49%	-10%	-98%	-60%	-25%
CTC	-106%	-94%	-2%	-92%	-69%	-38%
CPM	-80%	-64%	5%	-112%	-50%	-17%

DCS = Design Concrete Strength

ACS = Actual Concrete Strength

The table shows that the average error measures diminished significantly when the various corrections were used, but the standard deviations changed much less. Further improvement in the predictions can only be achieved if this scatter can be reduced. Such a reduction is likely to require better monitoring or control of phenomena that are not accounted for fully in the present methods, such as relative humidity, girder shape (including volume/surface ratio), and more detailed material properties. Accounting for these phenomena would require much more detailed reporting of materials properties than is done in present practice, in which measurements are seldom taken of elastic modulus and creep coefficient, much less of more advanced properties. Furthermore, production plants would have to record temperature and relative humidity, and sophisticated algorithms would need to be developed to account for parameters such as the volume/surface ratio. The need for camber predictions more accurate than those described here would therefore have to be evaluated carefully before such an effort were to be undertaken.

CONCLUSIONS

A number of factors influence the camber of a prestressed concrete girder. The findings associated with the broad study of 146 girders from six bridges, based on camber measurements taken at the production facilities, are as follows:

- 1) *Inclusion of prestress losses in deflection calculation.* The current WSDOT procedure uses the AASHTO LRFD 2007 provisions. However, because WSDOT does not include prestress losses in the time-dependant camber calculations, the magnitude of the time-dependent losses does not affect the predicted camber. This is true regardless of the prestress loss prediction method used.
- 2) *Calibration of model coefficients.* The numerical model was calibrated by minimizing the error between the predicted and measured cambers for the set of 146 girders. The coefficients for concrete strength, Young's modulus, creep coefficient and prestress loss due to creep were adjusted to achieve the best fit. The primary findings with respect to those factors are
 - a) Concrete strength. On average, the measured concrete compressive strength exceeded the specified strength by 10 percent at release and 25 percent at 28 days. The excess strength at release was particularly large when the girder was cured for more than one day, as often happens over weekends.
 - b) Elastic modulus. For a given concrete strength at release, the value of the elastic modulus, E_{ci} , derived from the release camber measurements was, on average, higher than that predicted by the AASHTO LRFD code equations by approximately 15 percent. The value of E_{ci} obtained from the Snake Lake camber measurements at release was in close agreement with the values obtained from the materials tests on companion cylinders.
 - c) Creep coefficient. The second camber measurements, which included the effects of long-term camber changes, depended on E_c , C_c , and the time-dependent prestress losses. For a given method of predicting prestress loss (e.g., AASHTO LRFD 2007) the measured camber values could be matched almost equally well by using any one of many different pairs of factors for E_c and C_c . Selecting the factor for E_c from the release measurements led to a unique pair and, therefore, to a single value of C_c . The optimization resulted in a modification factor of 1.4 for C_c .
- 3) Additional factors that were not included in the modeling, but that contribute to the inaccuracy of prediction, are girder support locations, restraint by supports, measurement error, and environmental conditions such as relative humidity, ambient air temperature and temperature gradients.

At the Keys Road Bridge site, girder cambers were measured at several times during construction. Seven spans, with 13 girders per span, or 91 girders in all, were monitored. Cambers were predicted using the numerical model and the optimum factors described above. The following observations were made from the site measurements.

- 1) *Effect of support conditions.* Some girder ends were supported on oak blocks and then built in to partial-height diaphragms, while others were seated on elastomeric bearings. Girders supported on oak blocks at both ends deflected less than those that

- were supported on an elastomeric bearing at one end. This was true both when the temporary strands were released (prior to the girder's embedment in the partial diaphragm) and when the deck was cast (after embedment). The lower deflections were attributed to fact that the bottom flange of the girder was partially restrained against longitudinal movement. The restrained girders behaved as if they were 41 percent to 46 percent stiffer than those seated on elastomeric bearings.
- 2) *Changes in camber due to changes in loading.* A simple span model was used to predict camber change for the spans with one end on an elastomeric bearing. However, when the temporary strands were released the measured camber change was 21 percent larger than predicted, but when the deck was cast the change was 14 percent less than predicted. The former result suggests an end restraint with a negative stiffness and is anomalous. By contrast, the spans that were restrained at both ends in all cases suffered camber changes that were less than those predicted by using a simple span model. This is consistent with the existence of partial end restraint. Attempts to model the end restraint rationally showed that improbably large pier stiffnesses were needed to match the measured camber changes. More detailed site data and more sophisticated analytical modeling than was possible here are needed to resolve the discrepancies.
 - 3) *Creep deflection using the composite section after deck placement.* The time-dependent deflection after deck placement was approximately 0.4 in., on average. However, a large amount of scatter was observed in the data, with a coefficient of variation of 150 percent. Some results were unexpected. For example, of the interior girders, those with two ends restrained deflected more than those with only one end restrained. Choosing a simple but rational model to compute the deflection is not easy because the elastic deflection is controlled by the bare girder properties, but the girder is composite by the time that the creep occurs. The best prediction was obtained by using the composite section to compute a (fictitious) elastic deflection and multiplying that by the creep coefficient to give the creep deflection.

NOTATION

a = distance from end of girder to harping point of prestress

b = constant that changes the rate of increase

c = constant that changes the ultimate value

C_c = creep coefficient

$E_c(t)$ = modulus of elasticity of concrete (ksi)

e_{end} = average prestressing eccentricity at the end of the girder

e_{mid} = average prestressing eccentricity at midspan of the girder

$f'_c(t)$ = concrete compressive strength

$f'_c(28)$ = 28-day concrete compressive strength

I_g = moment of inertia of the gross concrete section about the centroid axis, neglecting the reinforcement (in⁴)

k_f = factor for the effect of concrete strength

k_{hc} = humidity factor for creep

k_{hs} = humidity factor for shrinkage

k_s = factor for the effect of volume-to-surface ratio

k_{td} = time development factor

K_1 = correction factor for source of aggregate (WSDOT uses $K_1 = 1.0$)

L = total length of girder

L_c = length of girder overhang

L_n = length of girder span between supports

t_a = age of concrete at time of load application (day)

t_{str} = time after concrete starts to gain strength

w_c = unit weight of concrete (kcf)

w_{sw} = linear self weight of girder

Δf_{pCD} = prestress loss due to creep of girder concrete between time of deck placement and final time (ksi)

Δf_{pCR} = prestress loss due to creep of girder concrete between transfer and deck placement (ksi)

Δf_{pES} = sum of all losses or gains due to elastic shortening or extension at the time of application of prestress and/or external loads (ksi)

Δf_{pLT} = losses due to long-term shrinkage and creep of the concrete, and relaxation of the steel (ksi)

Δf_{pRI} = prestress loss due to relaxation of prestressing strand between time of transfer and deck placement (ksi)

Δf_{pR2} = prestress loss due to relaxation of prestressing strand in composite section between time of deck placement and final time (ksi)

Δf_{pSD} = prestress loss due to shrinkage of girder concrete between time of deck placement and final time (ksi)

Δf_{pSR} = prestress losses due to shrinkage of girder concrete between transfer and deck placement (ksi)

Δf_{pSS} = prestress loss due to shrinkage of deck in composite section (ksi)

Δf_{pT} = total losses (ksi)

$\Delta_{MISDPAN}$ = the deflection at midspan relative to the support

$\Delta_{OVERHANG}$ = the deflection of the overhang relative to the support

Δ_{PS} = total camber due to prestressing force

Δ_{SW} = total camber due to self-weight relative to the end of the member

$\epsilon_{sh}(t)$ = concrete shrinkage strain at a given time (in./in.)

$\psi(t, t_a)$ = creep coefficient

REFERNECES

1. Naaman, Antoine E. *Prestress Concrete Analysis and Design: Fundamentals*. Second Edition. Techno Press 3000, Ann Arbor MI, 2004.

2. American Association of State Highway and Transportation Officials (AASHTO). *AASHTO LRFD Bridge Design Specifications - Customary U.S. Units/4th Edition/2007*, Washington, D.C., 2007.
3. PGSuper, Prestressed Girder SUPERstructure design and analysis software, V2.0.0. Washington State Department of Transportation, Texas Department of Transportation, BridgeSight Software, 2007.
4. Washington State Department of Transportation (WSDOT). Bridge and Structures Office. *Bridge Design Manual*. 2007.
5. Hupauf, Tony. Internal Report. University of Washington, 2006.
6. Tadros, Maher K., Nabil Al-Omaishi, Stephen J. Seguirant, James G. Gallt. *Prestress Losses in High-Strength Concrete Bridge Girders*. National Cooperative Highway Research Program (NCHRP) Report 496, Transportation Research Board, Washington D.C., 2003.